The Journal of Experimental Biology 211, 790-797
Published by The Company of Biologists 2008
doi:10.1242/jeb.014613

Oxygen profiles in egg masses predicted from a diffusion–reaction model

H. Arthur Woods[1,*] and Amy L. Moran[2]

[1]Division of Biological Sciences, University of Montana, Missoula, MT 59812, USA and [2]Department of Biological Sciences, Clemson University, Clemson, SC 29634, USA

*Author for correspondence (e-mail: art.woods@mso.umt.edu)

Accepted 8 January 2008

SUMMARY

We developed a novel diffusion–reaction model to describe spatial and temporal changes in oxygen concentrations in gelatinous egg masses containing live, respiring embryos. We used the model in two ways. First, we constructed artificial egg masses of known metabolic density using embryos of the Antarctic sea urchin *Sterechnius neumayeri*, measured radial oxygen profiles at two temperatures, and compared our measurements to simulated radial oxygen profiles generated by the model. We parameterized the model by measuring the radius of the artificial masses, metabolic densities (=embryo metabolic rate×embryo density) and oxygen diffusion coefficients at both ambient (–1.5°C) or slightly warmer (+1.5–2°C) temperatures. Simulated and measured radial oxygen profiles were similar, indicating that the model captured the major biological features determining oxygen distributions. Second, we used the model to analyze sources of error in step-change experiments for determining oxygen diffusion coefficients (*D*), and to determine the suitability of simpler, analytical equations for estimating *D*. Our analysis indicated that embryo metabolism can lead to large (several-fold) overestimates of *D* if the analytical equation is fitted to step-down-traces of central oxygen concentration (i.e. external oxygen concentration stepped from some high value to zero). However, good estimates of *D* were obtained from step-up-traces. We used these findings to estimate *D* in egg masses of three species of nudibranch molluscs: two Antarctic species (*Tritonia challengeriana* and *Tritoniella belli*; –1.5 and +2°C) and one temperate Pacific species (*Tritonia diomedea*; 12 and 22°C). *D* for all three species was approximately 8×10^{-6} cm^2 s^{-1}, and there was no detectable effect of temperature on estimated *D*. For the Antarctic species, *D* in egg masses was 70–90% of its value in seawater of similar temperature.

Key words: oxygen, diffusion coefficient, egg mass, metabolism, nudibranch, size, Antarctic, embryo.

INTRODUCTION

A common reproductive strategy among aquatic and marine animals is to embed embryos in gelatinous masses (Strathmann, 1987; Lee and Strathmann, 1998). For masses, unlike adults, O_2 delivery problems are defined by only a few parameters: egg-mass size and shape, embryo metabolic rate, and O_2 diffusion coefficients in egg-mass gel. This simplicity has attracted attention from those working both on marine systems (Strathmann and Chaffee, 1984; Cohen and Strathmann, 1996; Lee and Strathmann, 1998; Moran and Woods, 2007; Woods and Podolsky, 2007) and on amphibian egg masses (Seymour, 1994; Seymour and Bradford, 1995; Mitchell and Seymour, 2003). For all egg masses, however, predicting transient temporal and spatial profiles of O_2 in masses remains difficult. First, O_2 concentrations at particular points in space and time reflect a balance of diffusion and reaction; second, the kinetics of O_2 consumption in biological systems often are non-linear (i.e. Michaelis–Menten); and third, estimating O_2 coefficients is challenging, especially when O_2 is consumed by metabolic reactions. Defining time- and space-integrated O_2 histories of embryos is crucial to understanding O_2 limitation in nature, and to predicting how variation affects embryos over development.

Here we develop a model of how egg-mass size and shape, O_2 diffusion coefficient, and embryo metabolic rate jointly affect O_2 distributions in egg masses. We constructed the model to (1) predict full radial and temporal profiles of O_2 in egg masses, even with nonlinear (Michaelis–Menten) reaction kinetics, and (2) analyze sources of error in estimating O_2 diffusion coefficients from experimental data in which external step-changes in O_2 concentration were imposed on intact, living egg masses. Given information about mass size, embryo O_2 consumption rates, number of embryos per unit volume of egg mass ('embryo density'), and diffusion coefficients, the model predicts O_2 concentrations anywhere in the structure and at any future time after a change in external O_2 concentrations. The model may be broadly applicable to other biological situations, as the basic set of mechanisms (oxygen diffusion and consumption) is responsible for establishing oxygen profiles in other structures, including tumors (Braun and Beatty, 2007), engineered tissues (Brown et al., 2007), insect eggs (Woods et al., 2005), and vertebrate embryos early in development (Kranenbarg et al., 2000).

Model development

In the marine literature, a frequently used model calculates maximal egg mass size (thickness) at which central O_2 just goes to zero:

$$R_{\max} = \sqrt{\frac{FDC_{\mathrm{R}}}{M(N/V)}}, \quad (1)$$

where $R_{\max}$ is half the maximum egg-mass thickness, F is a shape factor (6 for a sphere, 4 for an infinite cylinder and 2 for an infinite sheet), D is the diffusion coefficient of O_2, C_{R} is the O_2 concentration at the surface of the egg mass, M is the metabolic rate of an embryo, and N/V is the number of embryos per unit volume (embryo density).

Although Eqn 1 has been quite useful (see Lee and Strathmann, 1998; Woods, 1999; Moran and Woods, 2007) (and others), it suffers from several shortcomings. First, it predicts neither transient O_2 concentrations arising from changing conditions nor O_2 concentrations in non-central areas. Second, implicit in the equation is the assumption that embryo metabolic rate is constant for all O_2 levels above zero. Although approximately true when the half-saturation constant is low, this assumption can lead to serious underestimates of R_{max} when it is not. The new model developed below provides a more flexible framework for tracking spatial and temporal changes in O_2 and for incorporating different kinds of reaction kinetics. Similar approaches to analyzing oxygen in egg masses, using both iterative numerical modeling and finite element analysis, have been described (Seymour and White, 2006).

Consider an infinite cylinder, in which mass transfer occurs in the radial direction only. Diffusive transport is described by:

$$\frac{\partial C}{\partial t} = D\frac{\partial^2 C}{\partial x^2}, \quad (2)$$

where C is concentration, D is diffusion coefficient, t is time, and x is distance (Crank, 1975) (see Table 1). In radial coordinates, this equation becomes:

$$\frac{\partial C}{\partial t} = D\frac{1}{r}\frac{\partial}{\partial r}\left(r\frac{\partial C}{\partial r}\right). \quad (3)$$

Various time-dependent and steady-state solutions to this equation are well known (Carslaw and Jaeger, 1959; Crank, 1975). An additional transformation, from O_2 concentration to partial pressure, may sometimes be desirable. The transformation can be done by substituting (into Eqn 3) partial pressure, P, for concentration, C, and substituting Krogh's coefficient of diffusion, K, for D, the diffusion coefficient of O_2 (K=$D\beta$ and β is oxygen solubility). K does a better job of describing how O_2 transport changes with temperature, because it takes into account temperature's effects on both diffusion coefficient (positive) and solubility (negative).

We add metabolic consumption of O_2 to the radial equation with an extra term:

$$\frac{\partial C}{\partial t} = D\frac{1}{r}\frac{\partial}{\partial r}\left(r\frac{\partial C}{\partial r}\right) - f(C), \quad (4)$$

where $f(C)$ takes on any biologically realistic shape. For first-order kinetics,

$$f(C) = kC, \quad (5)$$

where k is the reaction coefficient. Here, metabolic rate declines linearly to zero as available O_2 declines. For first-order kinetics, a number of analytical solutions are available for different idealized shapes (Crank, 1975). Another, non-linear possibility is Michaelis–Menten kinetics,

$$f(C) = V_{max}C / (K_m + C), \quad (6)$$

which asymptotes at V_{max} at high O_2 concentrations and falls rapidly to zero at concentrations below K_m, the half-saturation (Michaelis) constant. Many biological systems sustain more-or-less constant metabolic rates down to low O_2 concentrations (Yanigasawa, 1975; Palumbi and Johnson, 1982). For example, embryos of the sea urchin *Arbacia* have constant metabolic rates down to approximately 10% of air saturation (Tang and Gerard, 1932). However, for embryos in gelatinous masses, gel and other materials around each embryo will act like large boundary layers for local diffusion, which may make the reaction kinetics appear more first-order. We explore both types of kinetics below.

Table 1. Definitions and units of terms used in model development

	Definition	Units
a	Radius of cylinder or sphere	cm
β	Oxygen solubility	nmol cm^{-3} kPa^{-1}
C	Oxygen concentration	nmol cm^{-3}
D	Oxygen diffusion coefficient	cm^2 s^{-1}
k	First-order reaction coefficient	s^{-1}
K	Krogh's coefficient of diffusion	nmol cm^{-1} s^{-1} kPa^{-1}
K_m	Half-saturation (Michaelis) constant	nmol cm^{-3}
l	Half thickness of sheet	cm
P	Partial pressure of oxygen	kPa
r	Radial distance	cm
t	Time	s
V_{max}	Maximum reaction rate at saturation	nmol cm^{-3} s^{-1}
x	Distance	cm
τ	Approximate time to reach steady state	dimensionless

We solved the equations numerically using a program written in the R statistical package (v. 2.3.1) with standard 3-point center differencing for second-order terms. The program takes arbitrary initial O_2 distributions (radially symmetric) and, for a given cylinder size, O_2 diffusion coefficient, reaction kinetics and surface concentration of O_2 (which depends on temperature *via* the parameter β), calculates the radial profile of O_2 concentrations at future times. Central O_2 concentrations (r=0) are undefined in Eqn 4 and so were obtained by cubic-spline interpolation.

In numerical models tending to steady state, there is the question of when states are in fact steady. In cylindrical diffusion, the approximate time τ is given by:

$$\tau = a^2 / D, \quad (7)$$

where a is cylinder radius. Systems with high metabolic rates arrive at steady states in times $<\tau$.

First-order *versus* saturating reaction kinetics

Embryo metabolic rates must change as O_2 availability declines from full air saturation (the usual condition under which embryo metabolism is measured) to low or zero O_2 within egg masses. The model allows analysis of different relationships between oxygen and metabolic rate. In particular, it shows that for equivalent metabolic rates at air saturation (here assumed to be air saturation at 11°C in seawater), Michaelis–Menten kinetics draw O_2 down further than linear kinetics (Fig. 1), because high reaction rates are sustained at low O_2 concentrations. At high rates of O_2 consumption, moreover, Michaelis–Menten kinetics gives different profiles and, with high V_{max}, larger central areas of anoxia. Overall, though, profile shapes were not particularly different.

Relative influences of diffusion and reaction: when does reaction matter?

When reaction kinetics are first order, a dimensionless number,

$$\varphi = ka^2 / D, \quad (8)$$

can be used as a shortcut for determining when metabolism will significantly depress central O_2 levels. In general, when φ<0.1

metabolism does not affect central O_2; when $\varphi>1$, there is a large effect (Fig. 2); and for $0.1<\varphi<1$ the effect of metabolism on central O_2 is moderate. A similar dimensionless number can be used with Michaelis–Menten kinetics, e.g. $V_{max}a^2/DK_m$. However, because the effect of O_2 on metabolism is nonlinear, it is difficult to develop general rules of thumb.

Estimating diffusion coefficients from step-change experiments

Using opisthobranch egg masses, Cohen and Strathmann (Cohen and Strathmann, 1996) estimated O_2 diffusion coefficients in egg-mass gel by measuring central O_2 concentrations during an externally imposed step-change in O_2 concentration (from air-saturated to N_2-purged) (see also Seymour, 1994). Metabolic consumption by embryos was eliminated by microwaving masses briefly to a high temperature. In such a no-reaction situation, the time course of central O_2 concentrations in cylinders is described by (Crank, 1975):

$$\frac{C-C_1}{C_0-C_1} = 1 - \frac{2}{a}\sum_{n=1}^{\infty}\frac{\exp(-D\alpha_n^2 t)}{a_n J_1(a\alpha_n)}\,, \qquad (9)$$

where $J_1(x)$ is the Bessel function of the first kind of order one, and α_ns are roots of:

$$J_0(a\alpha_n) = 0\,. \qquad (10)$$

For equal but opposite step changes, the time courses are mirror images of one another. The Appendix gives equations for central O_2 levels in both plane sheets and spherical masses.

When O_2 is consumed, Eqn 9 is invalid: metabolic consumption accelerates the central loss of O_2 during the external step-down and retards its rise during the external step back up, and the shapes of the two curves may differ. Here we explore how much they differ and whether the type of reaction kinetics (linear or Michaelis–Menten) affects how O_2 is distributed. Because the estimates derived above are computationally intensive, we subsequently explore methods for correcting estimates of D fitted from simpler equations.

Consider first-order (linear) O_2 consumption. For $\varphi=1$ or 4 (moderate and large effects of metabolism, respectively; see Fig. 2), the equilibrium central O_2 levels in air-saturated water were high and low, respectively. In both cases, traces of central O_2 levels during external step-down were symmetrical with traces during external step-up (Fig. 3A). By contrast, Michaelis–Menten kinetics gave asymmetrical traces (Fig. 3B): O_2 levels during step-down fell faster than they rose during step-up, and the asymmetry was magnified at larger V_{max}. Thus, information about both equilibrium O_2 levels in air-saturated water, and relative asymmetry in central O_2 traces during step changes, can be used to evaluate whether metabolism *in vivo* is better represented by first-order or Michaelis–Menten kinetics. An example based on real O_2 traces is developed below.

A further goal was to use step-change data to estimate O_2 diffusion coefficients (D) for different egg masses under contrasting environmental conditions. Ideally, D would be calculated by fitting the full model (Eqn 4) to the data. This approach is feasible only if one has reliable measurements of embryonic metabolic rate. An easier approach, developed here, is to fit a simpler equation (e.g. Eqn 9) that does not incorporate embryonic O_2 consumption. Estimates of D from such an approach will be biased by *in situ* O_2 consumption, but these biases can be mathematically corrected.

We used Eqn 4 to simulate step-change data under both 1st-order and Michaelis–Menten kinetics. Simulated data sets were then used to compare simpler methods of estimating D to results from our fully fitted model. In particular, we fitted Eqn 9 (which ignores

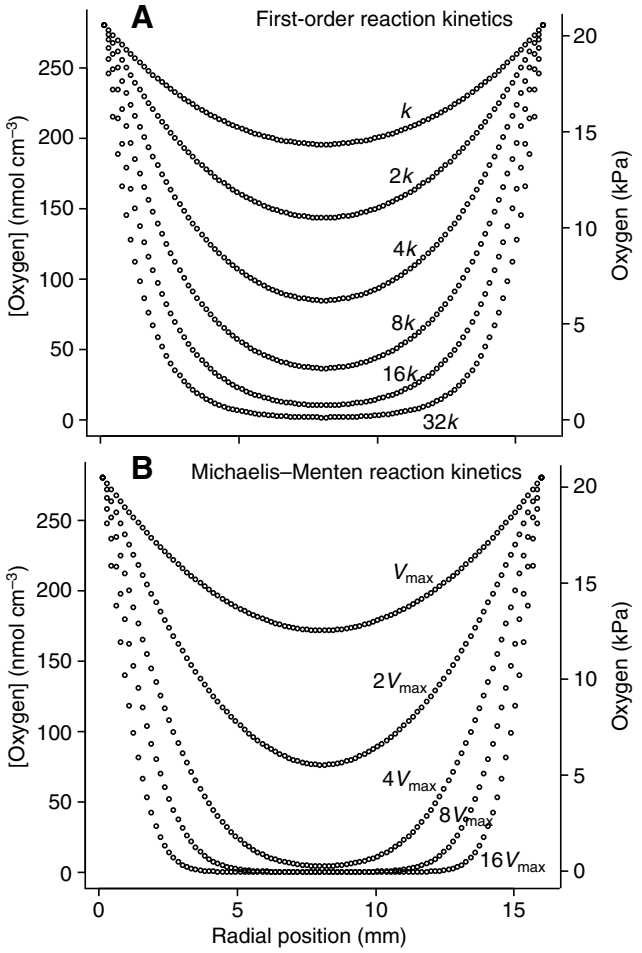

Fig. 1. Model predictions of steady-state O_2 profiles in cylindrical egg masses under two different kinds of reaction kinetics: (A) 1st-order and (B) Michaelis–Menten.

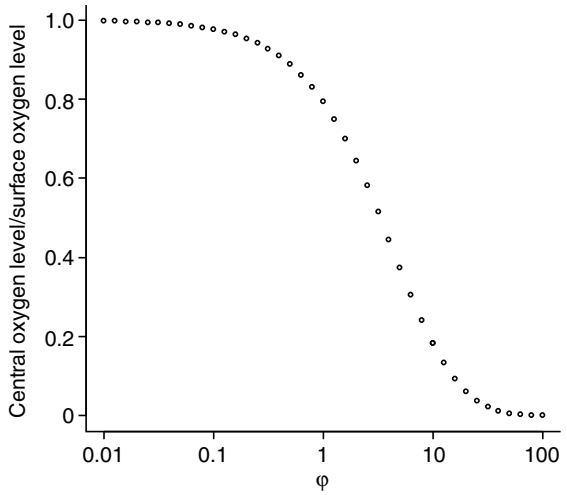

Fig. 2. Predicting the steady-state drawdown of O_2 in the middle of a cylindrical egg mass under first-order reaction kinetics. A dimensionless number, φ, incorporating information on the reaction coefficient, egg mass size and O_2 diffusion coefficient ($\varphi=ka^2/D$), predicts how far central O_2 levels will fall below surface concentration. At small φ, the relationship is transport-dominated; at large φ the relationship is metabolism-dominated.

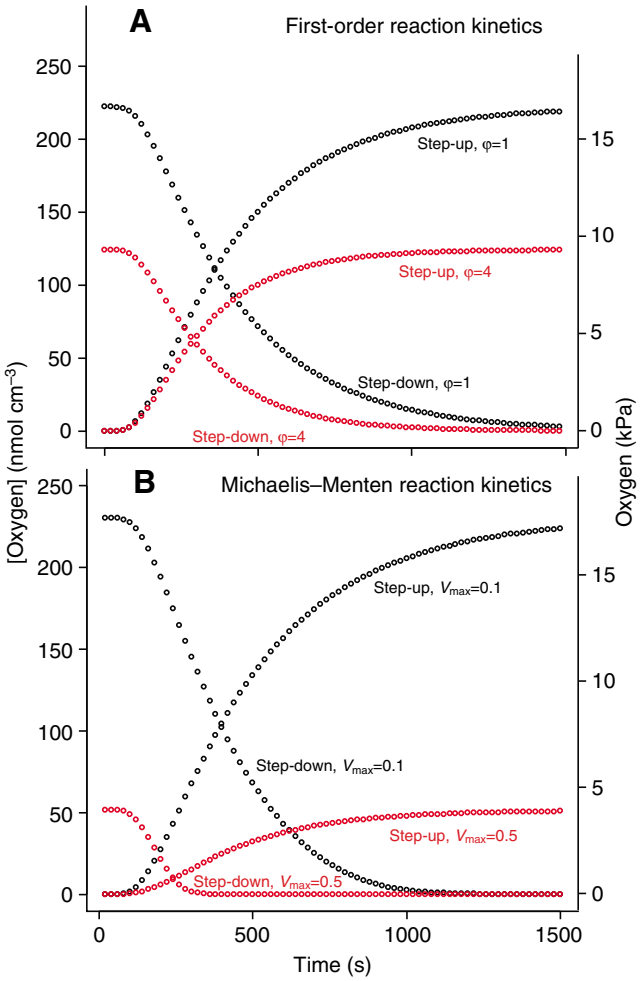

Fig. 3. Model comparisons of 1st-order (A) *versus* Michaelis-Menten (B) reaction kinetics on time courses of central O_2 concentrations during step-change experiments (i.e. external concentration changed from 280 to 0 nmol cm^{-3} and then *vice versa*). Under first-order reaction kinetics, larger φ gives larger initial drawdown (see Fig. 2), and the step-down and step-up-traces are always symmetrical. Analogously, under Michaelis–Menten kinetics, larger V_{max} gives greater initial drawdown. However, here the step-down and step-up-traces are asymmetrical, with the asymmetry exaggerated by larger initial drawdown.

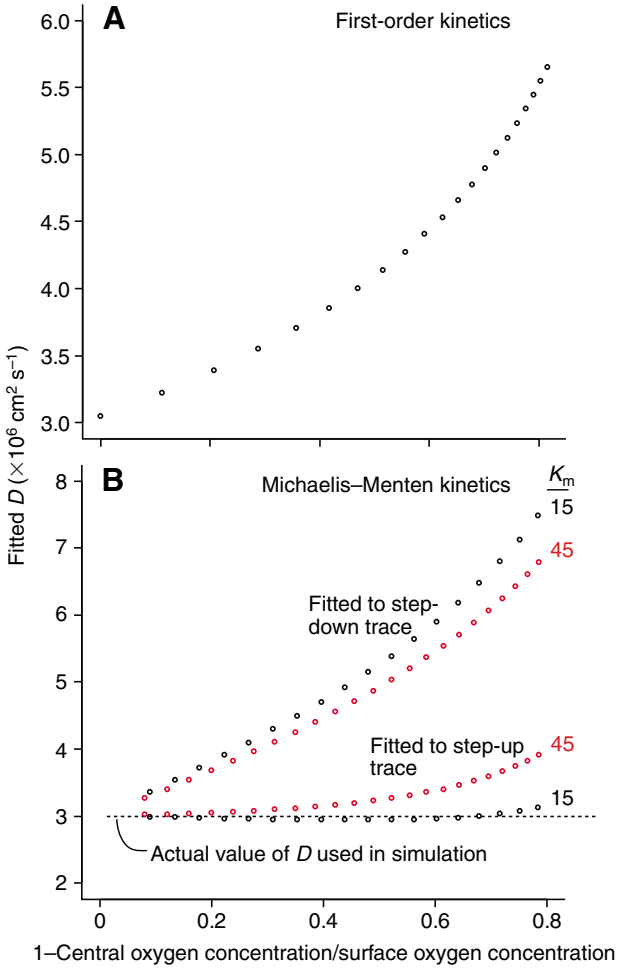

Fig. 4. Estimating *D* by fitting simple equations to complicated biological situations. When O_2 is consumed by metabolic processes, estimating *D* in biological structures is non-trivial, as metabolism draws down interior O_2 levels and alters the time course of change after external step changes. Here we simulated step change traces under both first-order and Michaelis–Menten reaction kinetics and then fitted a simple equation (Eqn. 9) to the simulated traces. Under first-order kinetics (A), estimated *D* was good when initial drawdown (or φ) was small. At higher *k*, giving greater initial drawdown, fitted *D* increasingly overestimated the known *D* used in the simulations (3×10^{-6}). Under Michaelis–Menten kinetics (B), estimated *D* was again good when initial drawdown was small. At higher V_{max}, giving greater initial drawdown, the down- and up-traces were highly asymmetrical. In this case, fitted *D* from the up-trace always gave values closer to the known, simulated value.

metabolism) to the traces, with the key assumption that the surface O_2 concentration at t=0 was equivalent to the central O_2 concentration at t=0. For first-order kinetics, data were simulated across a range of φ from 0 to 10, using $D=3\times10^{-6}$. Subsequent fits of Eqn 9 to data traces were done with the nonlinear least-squares function in R. As φ increased (increasingly high metabolic rate), estimated *D* (D_{est}) also rose; at φ=10, D_{est} was approximately twice *D*. To avoid having to estimate φ directly, it is also possible to use the depression of central O_2 level as a proxy (Fig. 4A). In a variety of simulated conditions, ~80% depression in central O_2 levels doubled estimated *D*.

Because step-down and step-up-traces are (under first order kinetics) mirror images, it is immaterial which trace is used to estimate *D*. Under Michaelis–Menten kinetics, by contrast, the step-down and step-up-traces have different shapes, and give different estimates of *D*. How to estimate the true value of *D*? We simulated central O_2 levels after step changes up or down using a range of V_{max} and either of two K_m values (15 or 45). The degree of divergence between down- *versus* up-estimates increased with V_{max} (Fig. 4B). Usually, however, up estimates were much closer to true simulated values than were down-estimates. In the model context, and likely too in real situations, these results suggest that *D* should be estimated by stepping from N_2-purged water to air-saturated water, rather than *vice versa*.

MATERIALS AND METHODS

Construction of artificial egg masses and model parameterization

To test the model, we made artificial egg masses (for details, see Moran and Woods, 2007) using ultra-low-melt agarose and fertilized embryos of the Antarctic sea urchin *Sterechinus neumayeri* (Meissner). Adult *S. neumayeri* were collected on SCUBA from

McMurdo Sound and returned to McMurdo Station, where they were spawned and gametes fertilized following Strathmann (Strathmann, 1987). Embryos were reared in stirred cultures of 0.5 μm filtered seawater at –1.5°C. When they were 4.5 days old (just prior to hatching), 10 ml of a known concentration of embryos was added to 20 ml of 2% ultra-low-gelling temperature agarose (Fluka BioChemika, Buchs, Switzerland; gelling temperature 4–6°C) cooled to 3°C with stirring. This solution was drawn into cylindrical molds, allowed to solidify, gently removed from the mold, and kept in –1°C running seawater tables until used.

We made masses of three diameters (3.4, 6.7 and 11.8 mm) and three densities (0, 1.25 or 12.5 embryos μl^{-1}) in a full-factorial design. Following published methods (Moran and Woods, 2007), we measured metabolic rates of 5-day-old embryos (from the same batch used to make artificial masses) at –1.5 and +1.5°C using a μBOD method and radial profiles of O_2 at –1.5 and +2°C using a Clark-style O_2 microelectrode (Unisense A/S, Aarhus, Denmark). In addition, O_2 diffusion coefficients in embryo-free masses were estimated using step-change experiments and fitting Eqn. 9 to traces of central O_2 concentration over time (see previous section; fits done using the R statistical package http://www.r-project.org). All measured parameters were put into the full numerical model (Eqn 4), assuming that embryos followed Michaelis–Menten kinetics. Modeled V_{max} was chosen so that it gave measured metabolic rates at air saturation. k_m was unknown but assumed to be low (=20 nmol O_2 cm^{-3}).

Estimating *D* in real egg masses

Artificial egg masses can be constructed without embryos, allowing straightforward estimation of diffusion coefficients from step-change experiments. Real egg masses are not so conveniently designed. One solution is to stop metabolism by killing embryos, e.g. by microwaving masses briefly to high temperature (Cohen and Strathmann, 1996). However, for cold-temperature Antarctic masses we were concerned that microwaving, exposure to high temperatures, or other chemical or physical means of killing embryos might affect gel structure and alter O_2 diffusion coefficients. Our model provides an alternative method to estimate *D* without killing embryos. To test the model in natural systems, we used egg masses of two congeneric nudibranch molluscs, *Tritonia diomedea* Bergh 1884 and *T. challengeriana* Bergh 1884, and of another Antarctic species, *Tritoniella belli* Bergh 1884. *T. diomedea* is common subtidally along the Pacific coast of North America. We collected adult *T. diomedea* on SCUBA in Puget Sound (WA, USA), primarily from Squamish Harbor, returned them to the Friday Harbor Laboratories, and kept them in running seawater tables (~11°C). Many individuals subsequently laid egg masses in the tables. We collected *T. challengeriana* and *Tritoniella belli* egg masses on SCUBA in McMurdo Sound, Antarctica, and kept them in running seawater tables (approx. –1°C) at McMurdo Station. Neither *Tritonia challengeriana* nor *Tritoniella belli* would lay egg masses in the laboratory, so we used field-collected masses. Positive identification of egg masses to species was made by observations of adults spawning in the field, and also by later observations of laboratory spawning events.

For all three species, we measured central O_2 concentrations using calibrated microelectrodes as described previously (Moran and Woods, 2007). After the microelectrode was positioned, egg masses were subjected to step changes in external O_2 concentration; the 'step-down' was a change from air-saturated to N_2 purged sea water, and the 'step-up' was from N_2 purged to air-saturated. Step changes were imposed by withdrawing chamber water into a syringe and immediately replacing it with temperature-equilibrated seawater (either N_2 purged or air-saturated, depending on the direction of the change). After a step-down, to avoid O_2 contamination, additional N_2 was bubbled into the egg-mass chamber and the water surface was isolated from the ambient air. After a step-up, air was bubbled into the chamber. Bubbling also stirred water around egg masses, thereby reducing boundary layers (Lee and Strathmann, 1998). Individual runs typically lasted 1 h (temperate measurements) or 3–4 h (Antarctic measurements). Drift from O_2 consumption by electrodes was negligible, as (i) equilibrium plateaus in egg-mass O_2 levels were very stable over time; (ii) the stirring effect, measured during calibration in bubbled *versus* still water, was 1–2% at most; and (iii) electrode tips consumed O_2 at rates well below rates measured for individual embryos in masses.

For all three species, paired pieces of individual egg masses (several cm long, cut ends tied with dental floss) were equilibrated in either cold or warm temperatures. For the temperate species, *T. diomedea* (*N*=7 paired mass pieces), the two experimental temperatures were 12°C and 22°C. For the Antarctic species, *T. challengeriana* (*N*=5 pairs) and *Tritoniella belli* (*N*=7 pairs), experimental temperatures were –1.5°C and + 2.0°C. Metabolic rate measurements of these species can be found in the accompanying paper (Woods and Moran, 2008b).

RESULTS

Application of the model to artificial egg masses

Measured radial profiles of O_2 (Fig. 5A) were largely symmetrical about egg mass centers, and the various factors had effects expected from our previous experiments with temperate artificial masses (Moran and Woods, 2007), namely that larger egg mass diameter, higher embryo densities and higher temperature all depressed central O_2 levels.

Metabolic rates of larval *S. neumayeri* were 8.6 and 10.3 pmol O_2 $larva^{-1}$ h^{-1} at –1.5 and +1.5°C, respectively. This difference corresponds to a Q_{10} of 1.8, and we used this value of Q_{10} to correct the higher metabolic rate to 2°C for use in the model, the temperature at which radial O_2 profiles were measured. Estimates of *D* from medium (6.7 mm) and large (11.8 mm) artificial masses gave values of 8.6×10^{-6} and 10.0×10^{-6} cm^2 s^{-1} at –1.5°C and +2°C, respectively. The known diffusion coefficient of O_2 in seawater at 0°C is 9.9×10^{-6} cm^2 s^{-1} (Denny, 1993).

Modeled radial profiles of O_2 (Fig. 5B) were remarkably similar to measured profiles (Fig. 5A). The main difference was that modeled profiles at +2°C were not quite as low as measured values.

Estimating *D* in real egg masses

Good fits were obtained by fitting the simple model (Eqn 9) to central O_2 concentrations in real egg masses (Fig. 6). In general, small initial O_2 depression gave symmetrical traces, and up- and down-traces gave similar estimates of *D*. By contrast, large initial O_2 depression gave both asymmetrical traces and much higher estimates of *D* for the down-trace than for the up-trace (see Fig. 3B). Across all three species at their two experimental temperatures, the relationship (Fig. 7) between initial O_2 depression and divergence in *D* was consistent with predictions of the full radial model with Michaelis–Menten reaction kinetics (see Fig. 4B). We estimated *D* in real egg masses of the three species using just up-traces (Fig. 8). Estimates of *D* were similar across species and temperatures, essentially always lying between $7–10\times10^{-6}$ cm^2 s^{-1}. However, temperature (warm *vs* cold within each species) had no statistically discernable effect on estimated *D* values, although the higher temperatures did tend toward higher *D*. *D* in egg masses of the two

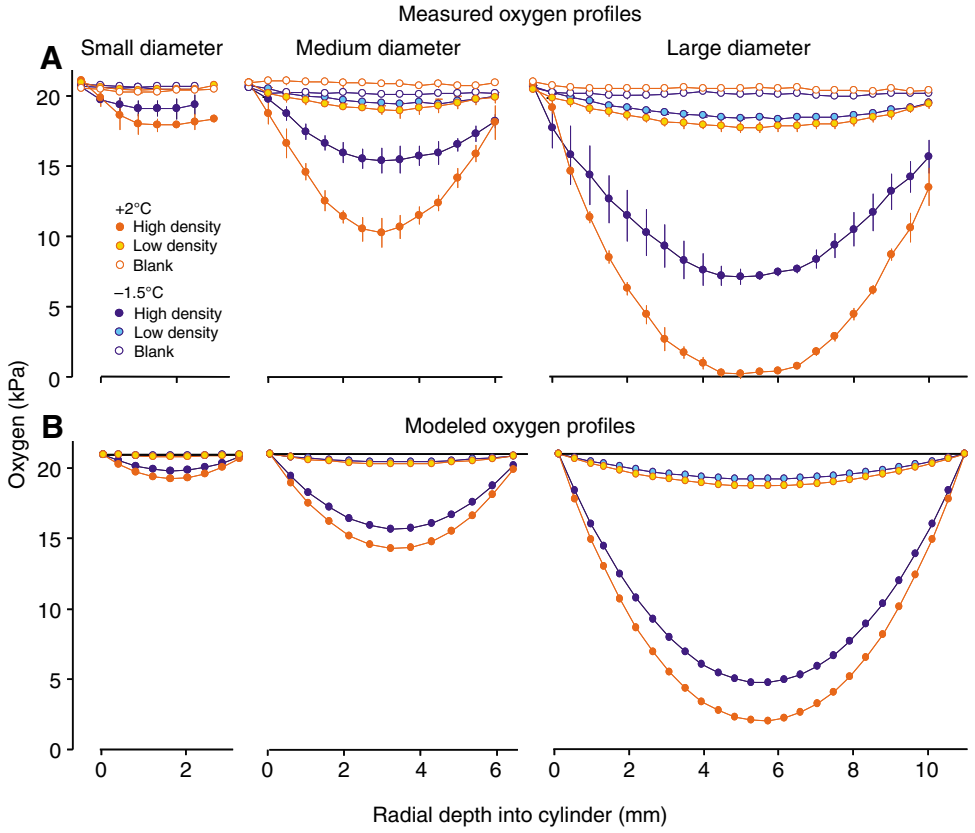

Fig. 5. Measured (A) and modeled (B) radial profiles of O_2 concentration in artificial egg masses. Masses were constructed from very low melting point agarose and 5-day-old fertilized embryos of the Antarctic sea urchin *Sterechinus neumayeri*. The model was parameterized using separately measured values of embryo metabolic rate, O_2 diffusion coefficient, cylinder size, and embryo density. In the model panels (B), horizontal black lines represent expected O_2 levels (air saturated throughout).

Antarctic species was very close to independently established values for D in pure seawater (9.9×10^{-6} cm^2 s^{-1}) (Denny, 1993). In the temperate species, *Tritonia diomedea*, estimated D values were less than half their values in seawater at the two (warmer) temperatures.

DISCUSSION

Application of the model to artificial egg masses

Measured and modeled radial profiles were remarkably similar, suggesting that the model is reasonable and that our measurements of its parameters were sufficiently accurate. Radial profiles in Antarctic artificial egg masses were qualitatively consistent with those found in artificial masses containing temperate sea urchin embryos that were measured at higher temperatures (13°C and 22°C) (Moran and Woods, 2007), in that greater mass diameter, higher embryo densities, and higher temperature all resulted in greater depression of central O_2 concentrations.

Estimating *D* in real egg masses

The logic and mathematics of estimating D in systems without metabolism are well developed. Most biological systems, however, violate the no-metabolism assumption to such an extent that simple mathematics are inadequate. How then should one estimate D? We approached this problem first by developing a full numerical model describing O_2 transport and consumption, with the option to specify different types of reaction kinetics. We then used the full model to simulate data that could be analyzed by simpler means. This approach showed that when Michaelis–Menten kinetics prevail, D is estimated accurately from the up-trace but not the down-trace.

We applied this conclusion to estimating O_2 diffusion coefficients in egg masses of three nudibranch species, *Tritonia challengeriana*,

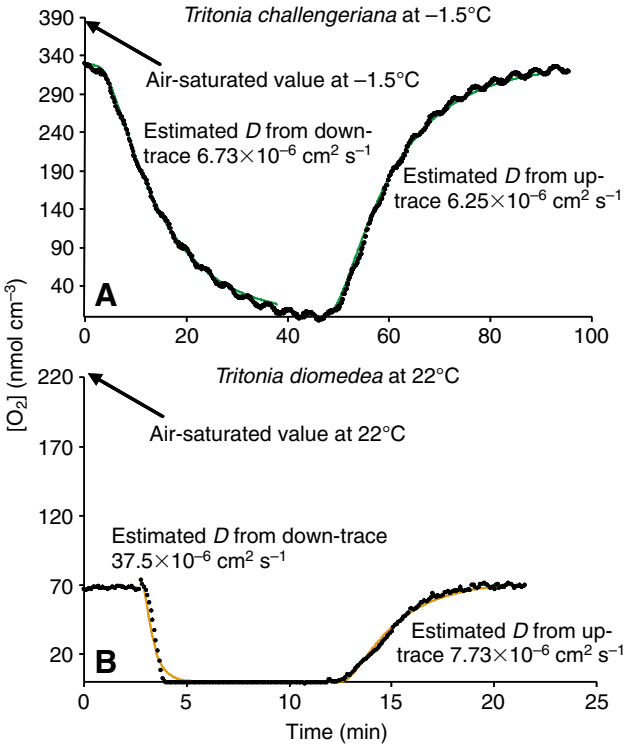

Fig. 6. Representative fits of Eqn 2 to central O_2 concentrations in an egg mass (A) with little initial O_2 depression (*Tritonia challengeriana* egg mass at –1.5°C; fits shown in green) or (B) with substantial initial O_2 depression (*Tritonia diomedea* egg mass at 22°C; fits shown in orange). *x*- and *y*-axes are scaled differently in the two panels. When initial drawdown is slight, estimates of D from down- and up-traces are similar, whereas when initial drawdown is large they are divergent (see also Fig. 7).

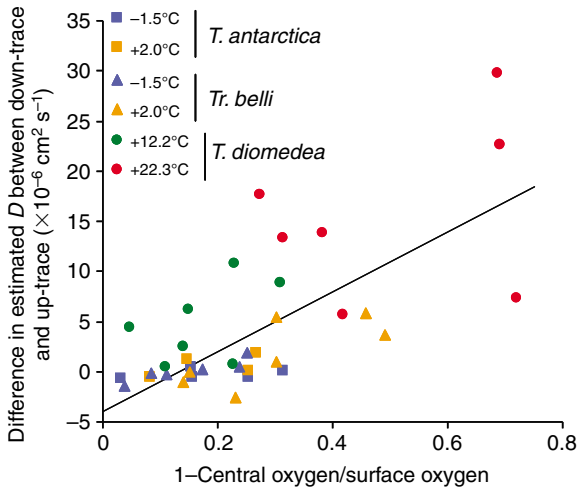

Fig. 7. Divergence in estimated D from down- and up-traces as a function of initial O_2 depression. As initial depression increased, traces became progressively more asymmetrical, leading to larger differences in estimated D. Regression line (y=3×10^{-5}x–4×10^{-6}) was fitted to the pooled data set.

Tritonia diomedea and *Tritoniella belli*. Down- and up-traces were highly asymmetrical, indicating that metabolism was better described by Michaelis–Menten than first-order kinetics. From up-traces only, D values for all three species were estimated to be ~8×10^{-6} cm^2 s^{-1}. Our analysis shows that potential errors from using down-traces to estimate D can be large. Fig. 7 shows that the divergence in estimates of D between down- and up-traces increases approx. linearly with degree of initial O_2 depression. At the highest levels of depression (e.g. only 25% of air saturation), estimates of D from down-traces were 15–20×10^{-6} cm^2 s^{-1} higher than from up-traces (~9×10^{-6} cm^2 s^{-1}), i.e. overestimated by 200–300%.

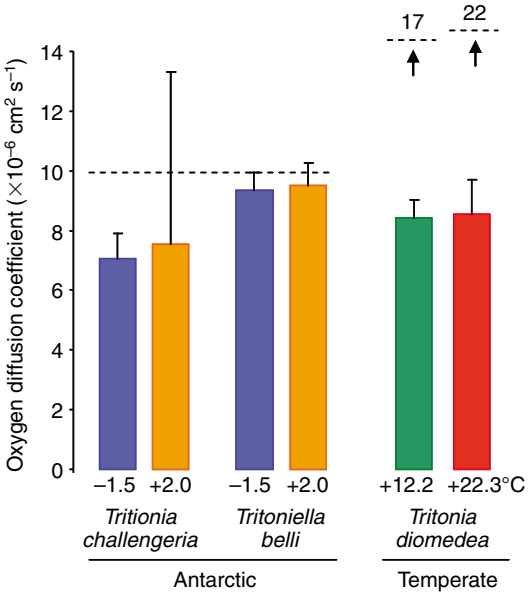

Fig. 8. Estimated O_2 diffusion coefficient (D) in egg masses of the three species in this study. Paired pieces of egg masses of *Tritonia challengeriana* and *Tritoniella belli* were subjected to either –1.5 or +2.0°C, and egg masses of *Tritonia diomedea* were subjected to 12.2 or 22.3°C. The longer broken line represents the O_2 diffusion coefficient in seawater at 0°C, and the two shorter lines are for the two warmer temperatures. Values are means ± s.e.m. (N=5–7).

The fitted values of D (Fig. 8) suggest two biological conclusions. First, egg-mass material itself does not depress O_2 diffusion coefficients much below their values in seawater, particularly in the two Antarctic species. This result matches Cohen and Strathmann's finding (Cohen and Strathmann, 1996) that D in egg masses of the opisthobranch *Melanochlamys diomedea*, at 20°C, ranged between 15 and 20×10^{-6} cm^2 s^{-1} (75–95% of the value of D in seawater at 20°C). Interestingly, D for *M. diomedea* was higher than the values we obtained here for *T. diomedea* at 22°C (~9×10^{-6} cm^2 s^{-1}). Why egg masses of the *T. diomedea* did not have higher D is unclear.

Second, in none of the three species did temperature have any substantial effects on D. One could object that a temperature change from –1.5 to 2°C would be unlikely to have dramatic effects anyway. However, other measurements of embryo metabolic rates [reported in the accompanying paper (Woods and Moran, 2008)] showed that, for at least some Antarctic species, such small temperature shifts stimulated metabolism two- to threefold, which was equivalent to the degree of metabolic stimulation that we found across a 9°C increase for the temperate embryos of *T. diomedea* (Moran and Woods, 2007). Also, here we measured D in egg masses of *T. diomedea* across the larger temperature increment and found no statistically significant effect. It thus appears that O_2 diffusion coefficients in egg-mass gel are relatively insensitive to temperature.

These data support the idea that changing temperature has larger effects on metabolic consumption than on diffusive transport of O_2 (Woods, 1999). This assumption stems from known physical effects of temperature on diffusing molecules: all else being equal, temperature will have only a weakly positive effect on diffusive transport. In biological systems, however, all else may not be equal; in particular, increasing temperature could alter physical or chemical properties of the matrix through which diffusion occurs. For egg masses, however, our findings here support the assumption that simple, physical models of temperature's effects on diffusion are adequate.

APPENDIX

The equations developed in the text apply to cylindrical egg masses – i.e. structures in which diffusive mass transport is radial. However, egg masses of particular species may be better approximated as plane sheets (e.g. dorid nudibranch masses) or spheres (e.g. the globular egg masses of the opisthobranch *Melanochlamys diomedea*). Here, following Crank (Crank, 1975), we lay out equations for these two other idealized shapes. Other solutions are available for variations on the scenarios below (Carslaw and Jaeger, 1959; Crank, 1975).

Plane sheets

For an infinite sheet of thickness 2l, initially at uniform concentration C_0 (in $-l<x<l$) and the two surfaces kept at constant concentrations C_1, the solution is:

$$\frac{C-C_0}{C_1-C_0} = 1 - \frac{4}{\pi}\sum_{n=0}^{\infty}\frac{(-1)^n}{2n+1}\sin\frac{n\pi r}{a}$$

$$\exp[-D(2n+1)^2\pi^2 t/4l^2]\cos\frac{(2n+1)\pi x}{2l}. \quad \text{(A1)}$$

Spheres

For a sphere with initial uniform oxygen concentration C_0 and surface concentration fixed at C_1, the solution is:

$$\frac{C - C_0}{C_1 - C_0} = 1 + \frac{2a}{\pi r} \sum_{n=1}^{\infty} \frac{(-1)^n}{n} \sin \frac{n\pi r}{a} \exp(-Dn^2\pi^2 t/a^2) . \quad \text{(A2)}$$

The central oxygen concentration is obtained by taking the limit as $r \rightarrow 0$:

$$\frac{C - C_0}{C_1 - C_0} = 1 + 2 \sum_{n=1}^{\infty} (-1)^n \exp(-Dn^2\pi^2 t/a^2) , \quad \text{(A3)}$$

which is a slightly rearranged version of the equation used by Cohen and Strathmann to estimate D from data on globose egg masses (Cohen and Strathmann, 1996).

We thank the directors and staffs of both the Friday Harbor Laboratories and McMurdo Station for support. SCUBA support was provided by two fearless Dive Safety Officers, Rob Robbins (McMurdo) and Pema Kitaeff (FHL), and their help is greatly appreciated. Others provided invaluable laboratory help and additional SCUBA assistance, including Bruce Miller, Jim Murray, Erika Schreiber and Jon Sprague. Two anonymous reviewers significantly clarified the manuscript. We also thank Dr Creagh Breuner and Dr Peter Marko for extraordinary logistical support while the authors were in Antarctica. This work was supported by the National Science Foundation (ANT-0440577 to H.A.W. and ANT-0551969 to A.L.M.).

REFERENCES

Braun, R. D. and Beatty, A. L. (2007). Modeling of oxygen transport across tumor multicellular layers. *Microvasc. Res.* **73**, 113-123.

Brown, D. A., MacLellan, W. R., Laks, H., Dunn, J. C. Y., Wu, B. M. and Beygui, R. E. (2007). Analysis of oxygen transport in a diffusion-limited model of engineered heart tissue. *Biotechnol. Bioeng.* **97**, 962-975.

Carslaw, H. S. and Jaeger, J. C. (1959). *Conduction of Heat in Solids* (2nd edn). Oxford: Oxford University Press.

Cohen, S. P. and Strathmann, R. R. (1996). Embryos as the edge of tolerance: effects of environment and structure of egg masses on supply of oxygen to embryos. *Biol. Bull.* **190**, 8-15.

Crank, J. (1975). *The Mathematics of Diffusion* (2nd edn). Oxford: Oxford University Press.

Denny, M. W. (1993). *Air and Water*. Princeton: Princeton University Press.

Kranenbarg, S., Muller, M., Gielen, J. L. W. and Verhagen, J. H. G. (2000). Physical constraints on body size in vertebrate embryos. *J. Theor. Biol.* **204**, 113-133.

Lee, C. E. and Strathmann, R. R. (1998). Scaling of gelatinous clutches: effects of siblings' competition for oxygen on clutch size and parental investment per offspring. *Am. Nat.* **151**, 293-310.

Mitchell, N. J. and Seymour, R. S. (2003). The effects of nest temperature, nest substrate, and clutch size on the oxygenation of embryos and larvae of the Australian moss frog, *Bryobatrachus nimbus*. *Physiol. Biochem. Zool.* **76**, 60-71.

Moran, A. L. and Woods, H. A. (2007). Oxygen in egg masses: interactive effects of temperature, age and egg-mass morphology on oxygen supply to embryos. *J. Exp. Biol.* **210**, 722-731.

Palumbi, S. R. and Johnson, B. A. (1982). A note on the influence of life-history stage on metabolic adaptation: the responses of *Limulus* eggs and larvae to hypoxia. In *Physiology and Biology of Horseshoe Crabs: Studies on Normal and Environmentally Stressed Animals*, pp. 115-124. New York: Alan R. Liss.

Seymour, R. S. (1994). Oxygen diffusion through jelly capsules of amphibian eggs. *Israel J. Zool.* **40**, 493-506.

Seymour, R. S. and Bradford, D. F. (1995). Respiration of amphibian eggs. *Physiol. Zool.* **68**, 1-25.

Seymour, R. S. and White, C. R. (2006). Models for embryonic respiration. In *Comparative Developmental Physiology: Contributions, Tools, and Trends* (ed. S. J. Warburton, W. W. Burggren, B. Pelster, C. L. Reiber and J. Spicer), pp. 41-57. Oxford: Oxford University Press.

Strathmann, M. F. (1987). *Reproduction and Development of Marine Invertebrates of the Northern Pacific Coast*. Seattle: University of Washington Press.

Strathmann, R. R. and Chaffee, C. (1984). Constraints on egg masses. II. Effect of spacing, size, and number of eggs on ventilation of masses of embryos in jelly, adherent groups, or thin-walled capsules. *J. Exp. Mar. Biol. Ecol.* **84**, 85-93.

Tang, P.-S. and Gerard, R. W. (1932). The oxygen tension-oxygen consumption curve of fertilized *Arbacia* eggs. *J. Cell. Comp. Physiol.* **1**, 503-513.

Woods, H. A. (1999). Egg-mass size and cell size: effects of temperature on oxygen distribution. *Am. Zool.* **39**, 244-252.

Woods, H. A. and Moran, A. L. (2008). Temperature–oxygen interactions in Antarctic nudibranch egg masses. *J. Exp. Biol.* **211**, 798-804.

Woods, H. A. and Podolsky, R. D. (2007). Photosynthesis drives oxygen levels in near-shore gastropod egg masses. *Biol. Bull.* **213**, 88-94.

Woods, H. A., Bonnecaze, R. T. and Zrubek, B. (2005). Oxygen and water flux across eggshells of *Manduca sexta*. *J. Exp. Biol.* **208**, 1297-1308.

Yanigasawa, T. (1975). Respiration and energy metabolism. In *The Sea Urchin Embryo* (ed. G. Czihak), pp. 510-549. New York: Springer.